



UNIVERSITY OF LEEDS

This is a repository copy of *Carbosilane terminated alkoxy cyanobiphenyls for bistable scattering mode LCDs*.

White Rose Research Online URL for this paper:

<https://eprints.whiterose.ac.uk/186089/>

Version: Accepted Version

Article:

Fritsch, L, Mandle, RJ orcid.org/0000-0001-9816-9661, Cowling, SJ et al. (1 more author) (2021) Carbosilane terminated alkoxy cyanobiphenyls for bistable scattering mode LCDs. *Journal of Materials Chemistry C*, 9 (2). pp. 714-718. ISSN 2050-7526

<https://doi.org/10.1039/d0tc05082b>

© The Royal Society of Chemistry 2021. This is an author produced version of an article published in *Journal of Materials Chemistry C*. Uploaded in accordance with the publisher's self-archiving policy.

Reuse

Items deposited in White Rose Research Online are protected by copyright, with all rights reserved unless indicated otherwise. They may be downloaded and/or printed for private study, or other acts as permitted by national copyright laws. The publisher or other rights holders may allow further reproduction and re-use of the full text version. This is indicated by the licence information on the White Rose Research Online record for the item.

Takedown

If you consider content in White Rose Research Online to be in breach of UK law, please notify us by emailing eprints@whiterose.ac.uk including the URL of the record and the reason for the withdrawal request.



eprints@whiterose.ac.uk
<https://eprints.whiterose.ac.uk/>

Carbosilane Terminated Alkoxybiphenyls for Bistable Scattering Mode LCDs

Luma Fritsch^{1,2}, Richard J. Mandle^{2,3}, Stephen J. Cowling², John W. Goodby²

¹ Instituto de Química, Universidade Federal do Rio Grande do Sul, Porto Alegre, RS, Brazil

² Department of Chemistry, University of York, York, UK, YO10 5DD

³ School of Physics and Astronomy, University of Leeds, Leeds, UK, LS2 9JT

Abstract

We report the synthesis and characterisation of a family of cyanobiphenyl liquid crystals with varying alkyl chain length and a carbosilane (1,1,3,3-tetramethyldisilabutane) terminal group. These materials exhibit significant reductions in melting point compared to the analogous alkoxybiphenyls and related siloxanes. X-ray scattering studies demonstrate that the carbosilane unit affords control over the SmA layer structure similar to that reported for other bulky terminal units. We demonstrate a single pixel ion-doped SmA scattering device utilising a single carbosilane terminated cyanobiphenyl that is capable of operating at room temperature with an upper temperature range of over 80 °C.

Introduction

Smectic liquid crystals exhibit both orientational and various forms of long-range positional order, with molecules self-organising into diffuse layers. Of the many smectic variants that exist the smectic A (SmA) is the simplest, and features diffuse layers whose layer normal is perpendicular to the direction of preferred molecular orientation (Fig. 1). The SmA phase has received significant interest for its ability to be used in light-scattering displays when doped with an ionic additive;¹⁻⁴ SmA based scattering devices are bistable,⁵⁻⁷ do not require a back light, and so are low power, and can be made flexible.^{6, 8, 1-7, 9} In addition to finding use in displays this technology could also be used in smart windows,⁷ e-paper,⁸ and so forth.

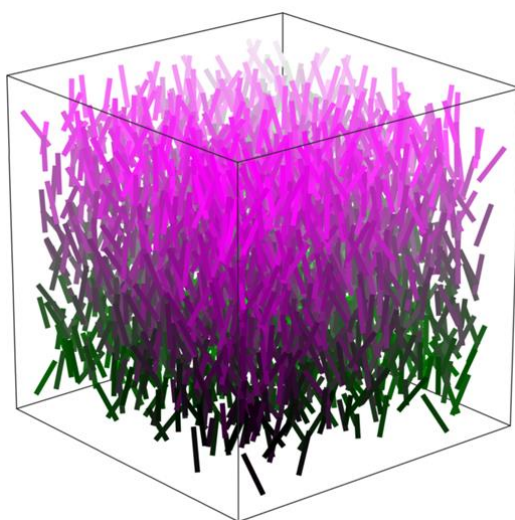


Figure 1: Depiction of the molecular organisation within the SmA phase; molecules are shown as rods, the colour of which is dependent upon their position along Z. The calculated scalar orientational order parameter ($\langle P_2 \rangle$) of this depiction is ~ 0.8 , typical for SmA phases of low molar mass materials.

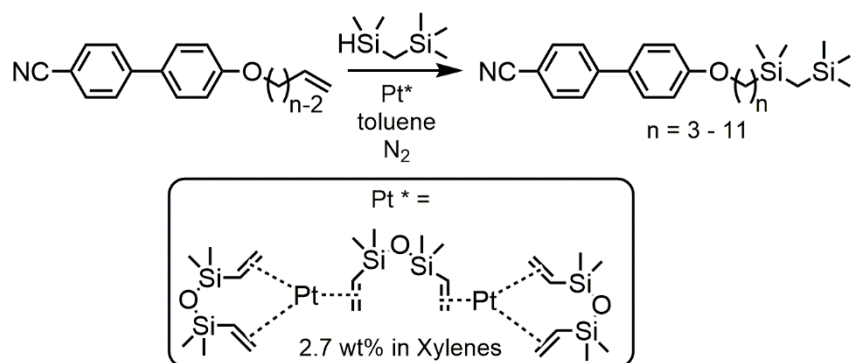
In terms of molecular design of SmA materials for display devices, much attention has been given to bulky terminal units as a means to control the local layered structure, reduce melting points, increase the temperature range of the SmA phase, and suppressing nematic phase formation.⁴ Terminal units such as halogens,^{10,11} (fluoro)phenoxy,¹² tert-butyl,¹³ have all been reported to exhibit some or all of these effects.

Terminal siloxanes are arguably the most successful example of a terminal group employed to lower melting points (relative to alkanes of equivalent length),³ with the added benefit that they suppress nematic liquid crystal phase formation,⁴ control smectic mesophase layer spacing,¹² and induce de Vries behaviour.¹⁴⁻¹⁸ Hydrosilylation, the addition of a silylhydride across an olefin, renders these materials synthetically trivial,¹⁹ however, there is also the serious problem of α and β addition resulting in small amounts of substitutional impurities. Furthermore, siloxanes have poor hydrolytic stability due to cleavage of the Si-O bond(s), affording silanols,²⁰ and are also labile in the presence of acids, bases and fluoride. Moreover, the relatively low purities of available siloxane building blocks tend to give liquid-crystalline materials of low purity; to this end we recently observed that the transition temperatures of siloxane terminated cyanobiphenyls prepared from highly purified alkenes and pentamethyldisiloxane under continuous flow conditions were significantly different from several literature examples.²¹

There is a growing body of literature surrounding the use of so-called 'carbosilanes' in liquid crystals.²² To a first approximation, carbosilanes can be considered simply to be siloxanes in which the oxygen atom(s) are replaced with methylene units. The requisite carbosilane precursors, e.g. 1,1,3,3-tetramethyl-1,3-disilabutane, are prepared easily from high purity and inexpensive chemical precursors,²³ and have excellent chemical stability due to the absence of a labile Si-O bond. While there is a growing body of literature focused on carbosilanes in de Vries type liquid crystals for SmC* based displays,^{18, 24-27} there are however few examples of carbosilanes utilised SmA materials targeted towards light scattering LCDs.¹² Given the advantages conferred by these end groups, this present study into the use of carbosilanes as terminal units in SmA materials for such devices is timely.

Experimental

The carbosilane terminated cyanobiphenyls were prepared as shown in Scheme 1. The alkene-terminated 4-alkoxy-4'-cyanobiphenyls were prepared as described previously,²⁸ while 1,1,3,3-tetramethyl-1,3-disilabutane was prepared as described previously by Kerst *et. al.*²³ Karstedt's catalyst was purchased from Fluorochem UK, toluene was purchased from Fisher Scientific UK and purified according to previous method.¹² We confirmed the exclusive formation of the anti-Markovnikov addition product by ¹³C DEPT135 NMR; the secondary CH₃-CH(-Si...)-CH₂- present in the undesired α -product gives a resonance in positive phase, whereas this resonance in the desired β -product has a negative phase due to the primary -CH₂-(Si...). We observe only a negative phase resonance for the carbon adjacent to the carbosilane (including ¹³C-²⁹Si satellites), indicating quantitative formation of the β -addition product. Full details of synthetic procedures and instrumentation employed are given in the SI.

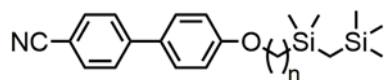


Scheme 1

Computational chemistry was performed using the wB97XD hybrid functional and the 6-31G(d,p) basis set as implemented in Gaussian G09.²⁹ Small- and wide- angle X-ray scattering (SAXS/WAXS) was performed using a Bruker D8 Discover equipped with a temperature controlled, bored graphite rod furnace, custom built at the University of York. The radiation used was copper K α ($\lambda = 0.154056$ nm) from a 1 μS microfocus source. Diffraction patterns were recorded on a 2048x2048 pixel Bruker VANTEC 500 area detector set at a distance of 121 mm from the sample, and calibrated against a silver behenate standard. Samples were filled into 0.9 mm O.D. capillary tubes (approx. I.D. ~ 0.85 mm, Capillary Tube Supplies Ltd, UK). The scattering pattern from an air filled capillary was used as a background. Background subtraction, radial integration and processing of raw X-ray scattering data contained within Bruker .gfrm files was performed in Matlab using scripts and functions developed in house.

Results and Discussion

The transition temperatures of compounds **1** – **9** were determined by differential scanning calorimetry (DSC), with phase assignment made by a combination of POM and X-ray scattering (SAXS/WAXS). The transition temperatures and associated enthalpies are presented in Table 1. While we use the numbering scheme **1** – **9** in this paper, we suggest these materials be referred to as [2SiC] n OCB in future, where n is the number of methylene units; i.e. compound **3** would become [2SiC]5OCB.



No.	n =		MP	T _G	SmA-Iso	d / Å
1 [2SiC]3OCB	3	T	14.5	-	34.0	20.19
		ΔH	4.2	-	2.9	
2 [2SiC]4OCB	4	T	-	-28.2	21.1	21.85
		ΔH	-	-	2.8	
3 [2SiC]5OCB	5	T	4.3	-31.1	51.3	22.72
		ΔH	12.3	-	3.7	
4 [2SiC]6OCB	6	T	-	-36.4	46.0	24.07
		ΔH	-	-	3.8	
5 [2SiC]7OCB	7	T	25.7	-	60.1	25.25
		ΔH	5.9	-	4.8	
6 [2SiC]8OCB	8	T	26.4	-	54.3	26.88
		ΔH	16.6	-	4.0	
7 [2SiC]9OCB	9	T	16.5	-	64.9	27.80
		ΔH	9.7	-	3.9	
8 [2SiC]10OCB	10	T	34.6	-	61.1	29.34
		ΔH	22.8	-	5.4	
9 [2SiC]11OCB	11	T	31.7	-	70.1	30.28
		ΔH	21.2	-	5.8	

Table 1: Transition temperatures (T, °C) and associated enthalpies of transition (ΔH, kJ mol⁻¹) for compounds **1** – **9**, as determined by DSC at a heat/cool rate of 10 °C min⁻¹. Molecular lengths, *d*, were calculated at the wB97XD/6-31G(dp) level of DFT³⁰. MP = melting point; T_G = glass transition. Data for compound **9** was taken from ref¹².

All nine materials exhibit enantiotropic smectic A phases, with phase identification confirmed by optical microscopy and X-ray scattering experiments. We performed SAXS experiments on unaligned samples of compounds **1**, **3-8** so as to study the local structure of the smectic A phase. Compound **2** exhibits the SmA phase only below ambient temperature, and so was not studied due to experimental limitations around sub-ambient temperature control. Data for compound **9** was published previously,

¹² and we make reference to this data here but do not reproduce it for reasons of brevity. Samples were cooled from the isotropic liquid in 1 °C steps until crystallisation or ambient temperature was reached (~ 26 °C); data are plotted in Fig. 2. For each material we find the layer spacing is temperature dependant, increasing as the temperature decreases. At any given reduced temperature the layer spacing is larger for materials with longer alkyl chains, as anticipated due to the increased molecular length. Using molecular lengths for compounds **1** – **9**, obtained from geometry optimised at the wB97XD/6-31G(dp) level of DFT,³⁰ we converted the layer spacing to a d/l ratio so as to facilitate comparison between materials of differing length. When considering the layer spacing as a d/l ratio we find only a small difference between each material at a given reduced temperature, each material having a d/l ratio in the range 1.65 – 1.75.

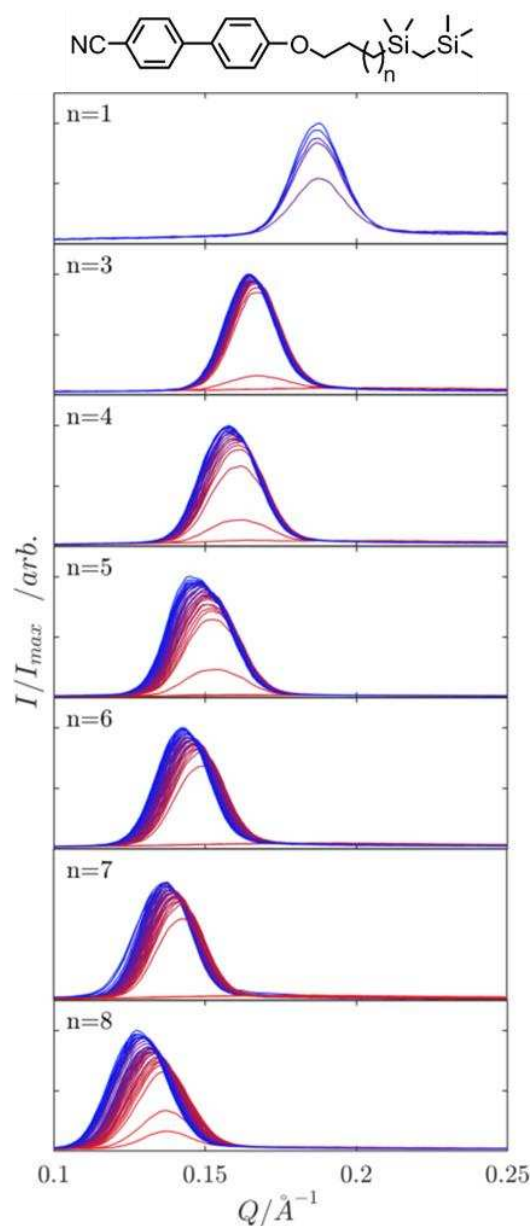


Figure 2: Plots of scattered intensity (I / I_{max} , arbitrary units) as a function of the scattering vector (Q , \AA^{-1}) for compounds **1**, **3-8**, with shortest chain length shown at the top and longest chain length

presented at the bottom. Within each plot a colour gradient is used to indicate temperatures, with red being highest and blue being lowest.

Given the structural similarity of the 1,1,3,3-tetramethyldisilabutyl end unit with pentamethyldisiloxane, a comparison of the liquid crystalline properties of these materials is logical. Transition temperatures for compounds **1** – **9**, along with the corresponding analogous pentamethyldisiloxanes, are plotted as a function of chain length in Fig. 3. We find clearing points to be comparable, but slightly lower for carbosilane terminated materials than siloxane (mean $\Delta T = 5.5$ °C), whereas melting points are significantly lower for carbosilane terminated compounds than the analogous siloxane (mean $\Delta T = 30.0$ °C); the slight reduction in clearing point is more than offset by the reduction in melting point.

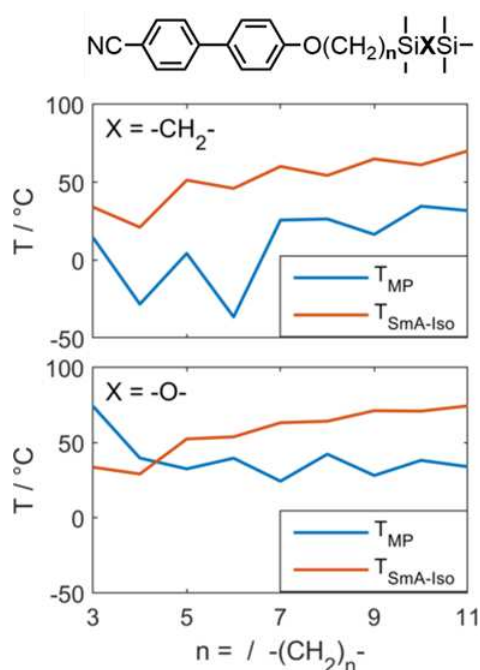


Figure 3: Plots of the transition temperatures (°C) of compounds **1-9** (X = -CH₂-, top) taken from this work, and of the analogous siloxanes (X = -O-, bottom). Data for siloxanes was taken from ref ²¹

As discussed in the introduction, our interest in extending the smectic A phase range of cyanobiphenyls is motivated by their possible device use. In order to assess behaviour under applied fields we selected one material for study (**4**), which was then doped with 0.05 wt% of hexadecyltrimethylammonium perchlorate (HTAP). Commercially available glass cells with ITO electrodes (10 mm² active area) with surfaces treated for homeotropic alignment (Instec, cell gap 5 ± 0.1 μm) were filled by capillary action at atmospheric pressure with **4**+HPAP heated into the isotropic liquid. The cells were cooled to ambient temperature, measured to be 22 °C, and allowed to stand for 24 hours.

A Hewlett Packard 33120A waveform generator and a custom-built linear ×20 amplifier were used to apply voltages to the cell. A 90 V square wave at a frequency of ca. 50 Hz gave a scattering state, whereas subsequent application of 90 V square wave at a higher frequency of 1 kHz gave a clear state. UV-visible absorption spectra of the devices in both states were recorded at ambient temperature (22 °C) using a Shimadzu UV-2401 PC spectrophotometer using air as a reference, with

an iris used to restrict the beam to the active area of the cells (10 mm²). As shown in Fig. 4, the 'clear' and 'scattering' states have significantly different transmittance, indicating the potential of these materials to be employed in scattering devices. Both the clear and transmitting state persist upon removal of the applied field. The cell was left in the clear state, and re-examined spectroscopically at 3- and 6- months to check transmittance, however the recorded spectra was almost indistinguishable from that recorded immediately after switching to the clear state (Fig. SI-1), with the transmittance dropping less than 0.5 % over this time. There is a small wavelength dependency upon transmittance in both states, note that the absorbance of light by the 4-cyanobiphenyl unit leads to effectively zero transmittance at and below a wavelength of 330 nm. It is worth noting that thicker cells will lead to improved scattering (lower transmittance) at the cost of increased drive voltage, whereas thinner cells offer voltage reduction at the cost of reduced scattering (higher transmittance).

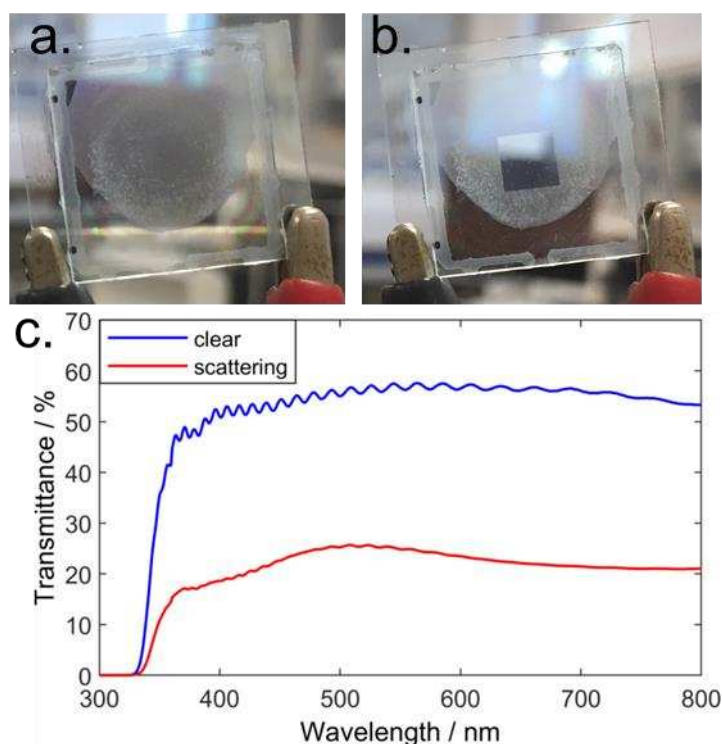


Figure 4: Scattering mode LCD using compound **4** doped with 0.05 wt% HTAP: photographs of (a) the scattering state, (b) the clear state; (c) transmittance spectra of the active area of the cell in the clear (blue) and scattering states (red).

Lastly we sought to demonstrate that larger quantities of material can be prepared easily using continuous flow hydrosilylation of 4'-(11-hydroxyundecyloxy)-4-cyanobiphenyl and 1,1,3,3-tetramethyldisilabutane (to afford compound **9**) using a Karstedt-like platinum-on-silica catalyst (Fig.5).^{21, 31} A reagent concentration of 0.2 M and a flow rate of 0.5 ml min⁻¹ gave effectively quantitative hydrosilylation; the only purification being removal of the volatiles (toluene and 1,1,3,3-tetramethyldisilabutane) *in vacuo* to yield **9** as a viscous liquid crystal, the properties and spectra of which were identical to an authentic sample prepared in a standard batch reaction. The throughput of this system is ~ 2.8 g hr⁻¹; this quantity being sufficient for around 30,000 single pixel devices such as that shown in Figure 4. High pressure pumps and back pressure regulation would allow larger

catalyst beds (therefore higher throughput) at the cost of increased cost and system complexity, negating the simple and inexpensive setup described.



Figure 5: Continuous flow hydrosilylation of 4'-(11-hydroxyundecyloxy)-4-cyanobiphenyl and 1,1,3,3-tetramethyldisilabutane using a platinum-on-silica catalyst ("Pt @ SiO₂").

Conclusions

A family of cyanobiphenyl liquid crystals with varying alky chain length and a 1,1,3,3-tetramethyldisilabutane end group – a ‘carbosilane’ – were synthesised. These materials exhibit significant reductions in melting point compared to the analogous siloxane materials, additionally this end group affords a similar control over the SmA layer structure as reported for other terminal units and leads to increased smectic layer spacings. We demonstrate a single pixel ion-doped SmA scattering device utilising a carbosilane terminated cyanobiphenyl prepared in this work.

Acknowledgements

The authors wish to thank the EPSRC for funding through grants EP/M020584/1 and EP/K039660/1. LF acknowledges funding by the Coordenação de Aperfeiçoamento de Pessoal de Nível Superior, Brazil (CAPES), finance code 001. Computational work was undertaken using the ARC4 machine, part of the High Performance Computing facilities at the University of Leeds, UK.

References:

1. C. Tani, *Appl Phys Lett*, 1971, **19**, 241-&.
2. D. Coates, W. A. Crossland, J. H. Morrissy and B. Needham, *J Phys D Appl Phys*, 1978, **11**, 2025-&.
3. D. J. Gardiner and H. J. Coles, *J Phys D Appl Phys*, 2006, **39**, 4948-4955.
4. D. J. Gardiner and H. J. Coles, *J Appl Phys*, 2006, **100**.
5. H. Y. Chen, R. Shao, E. Korblova, D. Walba, N. A. Clark and W. Lee, *J Soc Inf Display*, 2008, **16**, 675-681.
6. H. Y. Chen and J. S. Wu, *J Soc Inf Display*, 2010, **18**, 415-420.
7. K. Li, M. Pivnenko, D. P. Chu, A. Cockburn and W. O'Neill, *Liq Cryst*, 2016, **43**, 735-749.
8. Y. Lu, J. B. Guo, H. Wang and J. Wei, *Adv Cond Matter Phys*, 2012, DOI: 10.1155/2012/843264, 843264.
9. S. Khosla, K. K. Raina and H. J. Coles, *Curr Appl Phys*, 2003, **3**, 135-140.
10. I. Rugar, K. M. Mulligan, J. C. Roberts, D. Nonnenmacher, F. Giesselmann and R. P. Lemieux, *J Mater Chem C*, 2013, **1**, 3729-3735.
11. E. J. Davis, R. J. Mandle, B. K. Russell, P. Y. Foeller, M. S. Cook, S. J. Cowling and J. W. Goodby, *Liq Cryst*, 2014, **41**, 1635-1646.
12. R. J. Mandle, E. J. Davis, C. C. A. Voll, D. J. Lewis, S. J. Cowling and J. W. Goodby, *J Mater Chem C*, 2015, **3**, 2380-2388.
13. M. T. Sims, L. C. Abbott, J. W. Goodby and J. N. Moore, *Soft Matter*, 2019, **15**, 7722-7732.
14. J. C. Roberts, N. Kapernaum, F. Giesselmann and R. P. Lemieux, *J Am Chem Soc*, 2008, **130**, 13842-13843.
15. G. Galli, M. Reihmann, A. Crudeli, E. Chiellini, Y. Panarin, J. Vij, C. Blanc, V. Lorman and N. Olsson, *Mol Cryst Liq Cryst*, 2005, **439**, 2111-2123.
16. L. Li, C. D. Jones, J. Magolan and R. P. Lemieux, *J Mater Chem*, 2007, **17**, 2313-2318.
17. F. Goc, C. Blanc, V. Lorman, M. Nobili, S. Samaritani, G. Galli and W. Kuczynski, *Ferroelectrics*, 2006, **343**, 101-110.
18. Q. X. Song, D. Nonnenmacher, F. Giesselmann and R. P. Lemieux, *J Mater Chem C*, 2013, **1**, 343-350.
19. *United States Pat.*, 1972.
20. H. Ishida and J. L. Koenig, *J Polym Sci Pol Phys*, 1980, **18**, 1931-1943.
21. R. J. Mandle and J. W. Goodby, *Reaction Chemistry & Engineering*, 2018, **3**, 515-519.

22. C. Keith, R. A. Reddy, H. Hahn, H. Lang and C. Tschierske, *Chem Commun (Camb)*, 2004, DOI: 10.1039/b407890j, 1898-1899.
23. W. J. Leigh, R. Boukherroub and C. Kerst, *J Am Chem Soc*, 1998, **120**, 9504-9512.
24. C. P. J. Schubert, C. Muller, A. Bogner, F. Giesselmann and R. P. Lemieux, *Soft Matter*, 2017, **13**, 3307-3313.
25. K. M. Mulligan and R. P. Lemieux, *Liq Cryst*, 2015, **42**, 1229-1235.
26. C. P. J. Schubert, A. Bogner, J. H. Porada, K. Ayub, T. Andrea, F. Giesselmann and R. P. Lemieux, *J Mater Chem C*, 2014, **2**, 4581-4589.
27. K. M. Mulligan, A. Bogner, Q. X. Song, C. P. J. Schubert, F. Giesselmann and R. P. Lemieux, *J Mater Chem C*, 2014, **2**, 8270-8276.
28. R. J. Mandle and J. W. Goodby, *Liq Cryst*, 2017, **44**, 656-665.
29. M. J. Frisch, G. W. Trucks, H. B. Schlegel, G. E. Scuseria, M. A. Robb, J. R. Cheeseman, G. Scalmani, V. Barone, G. A. Petersson, H. Nakatsuji, X. Li, M. Caricato, A. V. Marenich, J. Bloino, B. G. Janesko, R. Gomperts, B. Mennucci, H. P. Hratchian, J. V. Ortiz, A. F. Izmaylov, J. L. Sonnenberg, Williams, F. Ding, F. Lipparini, F. Egidi, J. Goings, B. Peng, A. Petrone, T. Henderson, D. Ranasinghe, V. G. Zakrzewski, J. Gao, N. Rega, G. Zheng, W. Liang, M. Hada, M. Ehara, K. Toyota, R. Fukuda, J. Hasegawa, M. Ishida, T. Nakajima, Y. Honda, O. Kitao, H. Nakai, T. Vreven, K. Throssell, J. A. Montgomery Jr., J. E. Peralta, F. Ogliaro, M. J. Bearpark, J. J. Heyd, E. N. Brothers, K. N. Kudin, V. N. Staroverov, T. A. Keith, R. Kobayashi, J. Normand, K. Raghavachari, A. P. Rendell, J. C. Burant, S. S. Iyengar, J. Tomasi, M. Cossi, J. M. Millam, M. Klene, C. Adamo, R. Cammi, J. W. Ochterski, R. L. Martin, K. Morokuma, O. Farkas, J. B. Foresman and D. J. Fox, *Journal*, 2016.
30. J. D. Chai and M. Head-Gordon, *Phys Chem Chem Phys*, 2008, **10**, 6615-6620.
31. Q. J. Miao, Z. P. Fang and G. P. Cai, *Catal Commun*, 2003, **4**, 637-639.

US3814730A